HHS Public Access

Author manuscript

J Invest Dermatol. Author manuscript; available in PMC 2015 October 01.

Published in final edited form as:

J Invest Dermatol. 2015 April ; 135(4): 1043–1052. doi:10.1038/jid.2014.505.

Alpha actinin-1 regulates cell-matrix adhesion organization in keratinocytes: consequences for skin cell motility

Kevin J. Hamill[1,5], **Sho Hiroyasu**[2,5], **Zachary T. Colburn**[2], **Rosa V. Ventrella**[3], **Susan B. Hopkinson**[2], **Omar Skalli**[4], and **Jonathan C. R. Jones**[2]

[1]Department of Eye and Vision Science, Institute of Ageing and Chronic Diseases, the University of Liverpool, Liverpool, UK

[2]School of Molecular Biosciences, Washington State University, Pullman, WA

[3]Department of Dermatology, Feinberg School of Medicine, Northwestern University, Chicago, IL

[4]Department of Biological Sciences, University of Memphis, Memphis, TN

Abstract

The migration of keratinocytes in wound healing requires coordinated activities of the motility machinery of a cell, the cytoskeleton and matrix adhesions. In this study we assessed the role of alpha actinin-1 (ACTN1), one of the two alpha actinin isoforms expressed in keratinocytes, in skin cell migration via an shRNA-mediated knockdown approach. Keratinocytes deficient in ACTN1 exhibit changes in their actin cytoskeleton organization, a loss in front-rear polarity and impaired lamellipodial dynamics. They also display aberrant directed motility and move slower than their wild-type counterparts. Moreover, they have abnormally arranged matrix adhesion sites. Specifically, the focal adhesions in ACTN1 knockdown keratinocytes are not organized as distinct entities. Rather, focal adhesion proteins are arranged in a circle subjacent to cortical fibers of actin. In the same cells, hemidesmosome proteins arrange in cat paw patterns, more typical of confluent, stationary cells and β4 integrin dynamics are reduced in knockdown cells compared with control keratinocytes. In summary, our data suggest a mechanism by which ACTN1 determines the motility of keratinocytes by regulating the organization of the actin cytoskeleton, focal adhesion and hemidesmosome proteins complexes, thereby modulating cell speed, lamellipodial dynamics and directed migration.

Keywords

motility; lamellipodia; focal adhesion; hemidesmosome; integrin

Correspondence: Dr. Jonathan Jones, School of Molecular Biosciences, BLS 202F, Washington State University, 1770 NE Stadium Way, Pullman WA 99164, T: 509 335 8724, jcr.jones@vetmed.wsu.edu.

[5]Contributed equally to the design and implementation of this study

CONFLICT OF INTEREST

The authors state no conflict of interest

INTRODUCTION

Alpha actinins belong to a family of actin crosslinking proteins of which there are four major isoforms in mammals (Baron *et al*., 1987; Dixson *et al*., 2003; Parr *et al*., 1992; Youssoufian *et al*., 1990). Of these, alpha actinins-2 (ACTN2) and -3 (ACTN3) are expressed almost exclusively in muscle, while alpha actinins-1 (ACTN1) and -4 (ACTN4) display ubiquitous expression profiles (Beggs *et al*., 1992; Dixson *et al*., 2003; Honda *et al*., 1998; Millake *et al*., 1989; Parr *et al*., 1992; Youssoufian *et al*., 1990).

ACTN1 and ACTN4 are closely related at both the nucleotide and amino acid levels and each localizes to the lamellipodial extensions of motile cells (Honda *et al*., 1998; Sen *et al*., 2009; Yamaji *et al*., 2004). However, whereas ACTN1 localizes exclusively to the cytoplasm where it decorates and cross-links actin stress fibers, ACTN4 is found both in the cytoplasm and in the nucleus, where it activates transcription by binding to nuclear receptors under certain conditions (Babakov *et al*., 2008; Khurana *et al*., 2011; Khurana *et al*., 2012; Kovac *et al*., 2013; Vallenius *et al*., 2000). ACTN1 associates with the cytoplasmic domain of β1 integrin and, when phosphorylated, can interact with both focal adhesion kinase and the proto-oncogene tyrosine-protein kinase Src where it enhances signaling from matrix adhesion sites and stimulates integrin mediated cell to matrix adhesion (Craig *et al*., 2007). In addition, both ACTN1 and ACTN4 interact with collagen type XVII (Col XVII, bullous pemphigoid antigen 2), a transmembrane component of epithelial cell matrix adhesion devices termed hemidesmosomes (Craig *et al*., 2007; Gonzalez *et al*., 2001; Jones *et al*., 1998; Otey *et al*., 1990).

Recently we presented evidence that ACTN4 plays a role in regulating the directed migration of keratinocytes as well as the organization and dynamics of their cell-substratum attachments (Hamill *et al*., 2013). In contrast, the functions of its relative, ACTN1, in keratinocyte motility and matrix adhesion formation/organization are not known. In this regard, other studies indicate that the functions of ACTN1 in cellular migration are highly cell context dependent. For example, ACTN1 overexpression in 3T3 fibroblast cells leads to a reduction in cell motility rates while decreased ACTN1 expression increases cell motility and tumorigenicity (Gluck and Ben-Ze'ev, 1994). In contrast, in Gliobastoma Multiforme cells a decrease in ACTN1 expression correlates with decreased migration while in astrocytoma cells ACTN1 knockdown causes an increase in overall cell proliferation, but has no effect on cell motility (Quick and Skalli, 2010; Sen *et al*., 2009). The data we present in the current study indicate that knockdown of ACTN1 dramatically inhibits the motility of human epidermal cells and results in defects in their lamellipodial dynamics with concomitant changes in matrix adhesion.

RESULTS

Lentiviral-mediated shRNA knockdown of ACTN1 in human epidermal keratinocytes

Immortalized human epidermal keratinocytes (iHEKs) express two actinin isoforms, ACTN1 and ACTN4 (Figure 1a). Indirect immunofluorescence microscopical analyses reveal that ACTN1 antibodies not only decorate the leading lamellipodia but also stain filopidial-like extensions at the cell surface (Figure 1b). In contrast, ACTN4 localizes

primarily to the ruffles at the leading edge of lamellipodial extensions (Figure 1b)(Hamill *et al*., 2013).

To study the function of ACTN1 in epidermal cells we utilized lentivirus to deliver shRNA targeting ACTN1 to iHEKs. The lentiviral/shRNA constructs were previously characterized and validated (Quick and Skalli, 2010). Several clones were isolated and subsequently used for analyses. ACTN1 shRNA expressing clones –A, –B and –C exhibit 30%, 50% and 20%, respectively, of the ACTN1 expression levels of parental iHEKs and each shows dramatically diminished ACTN1 antibody staining (Figure 1a and b; a representative cell of one of three clones is shown). As a control for this and subsequent studies we derived iHEKs expressing a scrambled shRNA. The scrambled shRNA has no effect on ACTN1 protein expression or localization (Figure 1a and b). Moreover, the ACTN1 shRNA does not affect the levels of ACTN4, as shown by immunofluorescence and immunoblotting, showing that isoformspecific silencing was achieved (Figure 1a and b).

Actin and focal adhesion reorganization in ACTN1-knockdown cells

In front-rear polarized, single migrating iHEKs or iHEKs expressing scrambled shRNA, filamentous actin distributes in an arc behind the leading lamellipodium (Figure 2a). In all clones of iHEKs expressing ACTN1 shRNA, cortically arranged actin is observed around the entire cell edge with a loss in distinct front-rear polarity (Figure 2a).

We next evaluated the impact of ACTN1 knockdown on expression of focal adhesion components of keratinocytes. The cell surface levels of the focal adhesion-associated α3 integrin subunit is unaffected by ACTN1 knockdown as assessed by FACS (Figure 2b) (Carter *et al*., 1990). Total protein levels of the major focal adhesion proteins, paxillin, talin and vinculin remain unchanged in ACTN1-knockdown cells relative to control iHEKs. However, it should be noted that paxillin migrates as a more diffuse band in immunoblots of extracts of the knockdown cells, suggesting it may have undergone different post-translational modification compared to paxillin in control cells (Figure 2c).

In single, well-polarized control cells, punctate focal complexes and linear focal adhesions perpendicular to the cell edge are localized along the edge of the large, extended lamellipodium (Figure 2a; Supplementary Figure S1a and b). These are stained by antibodies against paxillin, FAK and α4 integrin (Figure 2a; Supplementary Figure S1a and b). Focal adhesions are also sometimes clustered at the rear of such cells. In ACTN1 knockdown cells focal adhesion protein components, including paxillin, α4 integrin and FAK, co-localize in complexes. However, in sharp contrast to control cells, these complexes are arranged in a ringlike band or a series of arcs towards the cell edge (Figure 2a; Supplementary Figure S1a and b). Few, if any, discrete focal adhesions are observed in such cells (Figure 2a; Supplementary Figure S1a and b).

Hemidesmosomal proteins in ACTN1-knockdown keratinocytes

In addition to focal adhesions, human keratinocytes assemble an immature hemidesmosome-like complex of proteins containing the bullous pemphigoid antigens (BPAG1e and collagen XVII), plectin and α6β4 integrin, involved in adhesion to substrate and motility (Carter *et*

al., 1990; Ozawa *et al*., 2010). ACTN4 knockdown has an impact on the localization of hemidesmosome protein-rich complexes in keratinocytes so we evaluated the impact of ACTN1 deficiency on the levels and organization of hemidesmosome components (Hamill *et al.*, 2013). In ACTN1-knockdown cells, levels of hemidesmosomal proteins and cell surface expression of β4 integrin are comparable to control iHEKs (Figure 3a and b; only β4 integrin and collagen XVII levels are shown). However, there are differences in the overall organization of hemidesmosomal proteins in control and knockdown single cells. In single, control iHEKs and iHEKs expressing scrambled shRNA, β4 integrin and collagen XVII are found mostly in punctate arrays arranged in arcs towards the edge of each individual cell (Figure 3c; Supplementary Figure S1c). In sharp contrast, in single cells in all the ACTN1 knockdown clones, β4 integrin and collagen XVII also organize into circular plaques/'cat paw' patterned areas towards the cell center, an arrangement more typical of that observed in groups of cells or confluent monolayers (compare Figure 3c; Supplementary Figure S1c and d). In such cell groups, hemidesmosome components co-distribute with each other mostly in cat paw, rosette and plaque-like patterns organized in a coordinated fashion across cell boundaries (Supplementary Figure S1d).

ACTN1-knockdown keratinocytes display impaired lamellipodial dynamics and cell motility

As mentioned above, our immunofluorescence analyses suggest that ACTN1 knockdown cells display polarity defects. To investigate this further, images of live individual cells plated overnight on glass-bottomed dishes were captured and cell surface area, lamellipodial area and number of lamellipodial protrusions were determined (Figure 4a). Although ACTN1 knockdown keratinocytes occasionally display slightly smaller cell body area than parental iHEK, the difference from controls is below significance (Figure 4b). In addition, their lamellipodial area, a combination of the area covered by their small multiple cell surface extensions, remains unchanged (Figure 4b). However, there is a significant decrease in ACTN1-knockdown lines exhibiting a single lamellipodium in comparison to control iHEKs (Figure 4c). This confirms that knockdown cells show a reduction in intrinsic frontrear polarity.

The observed changes in lamellipodial number in all the ACTN1-knockdown clones suggest that ACTN1 may be involved in the regulation of lamellipodial extension/protrusion. To test this, we analyzed lamellipodial dynamics by imaging individual keratinocytes every 5 seconds over 10 minutes and generated a kymograph of a 1-pixel-wide line drawn in the direction of the major lamellipodial protrusion (Figure 4d). From these kymographs, we determined, the time spent elongating (extension persistence), the length of the extension event (protrusion distance) and the ratio of distance/persistence (rate of extension) for each protrusion event. The lamellipodia of ACTN1-knockdown iHEKs have significantly reduced mean extension persistence and protrusion distance, with no significant difference on the rate of their extension (Figure 4d–g).

Reduced lamellipodial extension has been shown to correlate with reduced intrinsic directionality of gross migration (Hinz *et al*., 1999). To assess the motile behavior of ACTN1-knockdown cells, individual keratinocytes were imaged every 2 minutes over 1 hour and vector diagrams were plotted of the paths of cells over that time course

(representative plots in Figure 5a). Cells of all ACTN1-knockdown clones display a dramatic decrease in migration speed relative to controls (Figure 5b). The knockdown cells also exhibit decreased directed migration or processivity (Supplementary Figure S2a). To investigate this further, we also performed 'scratch' closure assays on confluent monolayers of ACTN1-knockdown cells, iHEK expressing scrambled shRNA and control iHEK. The knockdown cells close a scratch wound significantly slower than iHEK control cells and iHEK expressing scrambled shRNA, consistent with the single cell motility assays above (Figure 5c; results for only one clone shown).

To assess whether the above defects in motility of the knockdown cells are due to off-target effects of the ACTN1 shRNA, we rescued ACTN1 expression in the knockdown cells by infecting cells with adenovirus encoding ACTN1 mRNA refractory to the shRNA and tagged with GFP (Figure 5d). Knockdown cells expressing the GFP-tagged protein have normal appearing focal adhesions at the cell periphery (Figure 5e). Moreover, β4 integrin is displayed in arcs towards the cell edge and is not arranged in obvious circular plaques/cat paw patterns (Figure 5e; compare with Figure 3c). We detect expression of the tagged ACTN1 protein at 3–4 days post infection. In order to perform single cell motility assays the cells must be plated sparsely prior to analysis. However, the infected cells are highly sensitive to trypsin with fewer than 50% of passaged cells adhering to an uncoated substrate. In contrast, when infected cells are plated onto laminin-332-or fibronectin-coated substrates this problem is avoided with over 95% of the passaged cells adhering to and spreading on this substrate (Kligys *et al.*, 2012). Hence, we evaluated focal contact organization and the motility of control, ACTN1 knockdown and the rescued cells at 6–10 hours after plating onto laminin-332- coated substrates (Supplementary Figure S2b; Figure 5f and g). Interestingly, paxillin localizes in discrete entities in the knockdown cells plated onto both laminin-332- and fibronectin-coated surfaces and is not arranged in the same circles and arcs that we observe when the knockdown cells are plated onto uncoated surfaces (compare Figure 2a with Supplementary Figure S2b; quantification is shown in Supplemental Figure S2c). However, despite this apparent 'normalization' of focal contact organization, ACTN1 knockdown cells on a laminin-332-coated surfaces exhibit aberrant motility including decreased speed and directed migration when compared to iHEKs plated onto the same matrix, consistent with their aberrant motility on their 'own' matrix (Figure 5f and g; Supplementary Figure S2d). The same is true if the knockdown cells are plated onto a fibronectin-coated substrate (results not shown). On the other hand, the knockdown cells expressing ACTN1 mRNA refractory to the ACTN1 shRNA show comparable motility behaviors to iHEKs when plated on laminin-332-coated surfaces (Figure 5f and g; Supplementary Figure S2g). This is not the case when the same cells were induced to over-express tagged ACTN4 (result not shown). In both studies, cells expressing the refractory ACTN1 message or ACTN4 were identified by their GFP signal. Together these studies confirm that the ACTN1 knockdown phenotypes we detail with regard to motility are not due to off-target effects of the ACTN1 shRNA.

In addition, to rule out that the effects of ACTN1 knockdown on motility in iHEK are peculiar to this immortalized cell type we also infected primary human keratinocytes (pHEK) with lentivirus encoding ACTN1 shRNA. Pooled populations of the treated pHEK

exhibit a 40% reduction in ACTN1 protein levels and display the same aberrant polarity (Supplemental Figure S3a) and defective scratch wound closure behavior as their knockdown iHEK counterparts (Supplementary Figure 3b and c).

β4 integrin dynamics are impaired in ACTN1-deficient keratinocytes

The changes in organization of hemidesmosomal proteins into cat paw patterns in single cells following ACTN1 knockdown, led us next to study whether there is modulation in the dynamics of the hemidesmosome-specific β4 integrin in the knockdown cells. To undertake such analyses we infected cells lacking expression of β4 integrin with GFP-tagged β4 integrin protein. These cells, derived from a patient with junctional epidermolysis bullosa and induced to express the tagged integrin, have been described previously (Seghal *et al*., 2006; Hamill *et al*., 2013). The tagged protein localizes in a hemidesmosomal protein arrangement in the cells (Figure 6a). Furthermore, we knocked down ACTN1 in these cells (Figure 6b). Then we assayed β4 integrin dynamics in the knockdown cells using FRAP. There is a significant decrease in the dynamics of β4 integrin in the knock-down cells compared with controls as determined by FRAP (Figure 6a and c).

DISCUSSION

In the current study we focused on assessing the consequence of reduced ACTN1 expression on the motile behavior of keratinocytes. Our data indicate that loss of ACTN1 results in a dramatic slowing of cell motility. These results contrast with the consequences of ACTN4 knockdown which we recently presented (Hamill *et al*., 2013). In the latter instance, although the cells lose directionality, their speed is unaffected (Hamill *et al*., 2013). Indeed, together, the data here and in our earlier publication suggest that a primary function for ACTN1 is as a regulator of the “engine” of motility whereas ACTN4 chiefly functions as part of the “steering” mechanism of a keratinocyte.

In addition to and consistent with its effect on cell motility, ACTN1 knockdown has a profound impact on focal adhesion protein organization along the substratum-attached surface of a keratinocyte cell as well as the supramolecular structure of the actin cytoskeleton. Specifically, we also see punctate focal arrangements of actin in the knockdown cells suggesting that ACTN1 deficiency leads to actin cytoskeleton reorganization. More dramatic, there are few discrete focal adhesions in cells exhibiting ACTN1 knockdown when they are maintained on uncoated surfaces. Rather, focal adhesion components organize in a ring-like array towards the cell edge of the knockdown cells in close association with a rearranged cortical array of actin microfilaments. Intriguingly, although plating the knockdown cells on either laminin-332 or fibronectin-coated substrates fails to resolve the motility defects exhibited by the cells it corrects the localization of their focal adhesions. The mechanism underlying this correction is unclear although it likely reflects an aspect of inside-out signaling mediated by the matrix receptors expressed by keratinocytes (Hynes, 2002).

In addition to its effects on focal adhesion protein localization, knockdown of ACTN1 has a negative impact on the dynamics and induces changes in the localization of β4 integrin. Most likely this is due to the changes in the actin cytoskeleton induced by the knockdown

and is consistent with published data indicating that the actin cytoskeleton regulates the movements of α6β4 integrin complexes in the plane of the membrane (Tsuruta *et al.*, 2003). Moreover, the decrease in β4 integrin dynamics would explain the stabilization of the cell edges/lamellipodia in ACTN1knockdown cells since previous published data indicate that hemidesmosome proteins play an important role in regulating lamellipodial stability (Hamill *et al*., 2011a). With regard to hemidesmosome protein localization, in single ACTN1 knockdown cells hemidesmomal proteins are organized into the cat paw patterns and circles observed in non-motile multicellular groups. Indeed, their arrangement appears more typical of 'mature' hemidesmosome protein complexes, such as those in 804G bladder cells, at least in comparison to the cell edge-associated arcs observed in most control single keratinocytes (Riddelle *et al.*, 1991, 1992). One explanation is that this maturation phenomenon is a secondary consequence of the misorganization of focal adhesions and their associated actin cytoskeleton in ACTN1 knockdown cells, consistent with the notion that focal adhesions and hemidesmosome protein complexes crosstalk (Ozawa *et al*., 2010). However, we failed to see cat paw organizations of hemidesmosomal proteins in ACTN4 knockdown cells, despite there being changes in focal adhesion protein and actin distribution in the same cells (Hamill *et al*., 2013). Since the speed of ACTN1 knockdown cells is much slower than that of their wild type or ACTN4 knockdown counterparts, we suggest an alternate explanation for the apparent change in organization of hemidesmosome protein complexes in ACTN1 knockdown cells; the lack of motility of the cells facilitates maturation of hemidesmosomal matrix adhesions. This simple mechanism would explain why bona fide mature hemidesmosomes that firmly tether cells to their underlying matrix are only formed during wound healing once the wound has been completely epithelialized, despite the presence of their components at and around the leading tongue of moving keratinocytes prior to wound closure (Stock *et al.*, 1992; Martin, 1997; Underwood *et al.*, 2009).

In summary, our results indicate that iHEKs exhibiting reduced ACTN1 expression show profound motility defects consistent with changes in both the organization of their focal adhesions and actin cytoskeleton. In addition, the data we present here and those in our earlier publication emphasize the functional differences of actinin isoforms in keratinocytes (Hamill *et al*., 2013). Such differences are the likely explanation for why ACTN1 fails to compensate for the loss of ACTN4 and vice versa despite their molecular similarity (Dixson *et al*., 2003). Regardless, our data emphasize that actinin family members play key, distinct, regulator roles in keratinocyte motility, a process central to the epithelialization of wounds of the skin as well as dissemination of cells in skin tumors.

MATERIALS AND METHODS

Cell Culture, Lentivirus and Adenovirus

Immortalized normal human epidermal keratinocytes (iHEKs) and immortalized keratinocytes derived from a patient with junctional epidermolysis bullosa lacking β4 integrin expression, a generous gift of Dr. Peter Marinkovich, were maintained in defined keratinocyte serum-free medium supplemented with 1% penicillin/streptomycin mixture (Life Technologies., Carlsbad, CA, USA) and grown at 37°C (Seghal *et al*., 2006). ACTN1-knockdown iHEKs were generated using previously described lentiviral shRNAs (Quick and

Skalli, 2010). iHEKs (5×10^5) were seeded into 6-well plates overnight, then infected with shRNAs encoding ACTN1 or scrambled shRNA at a multiplicity of infection (MOI) of 0.5 in culture media supplemented with polybrene (8 μg/mL; Life Technologies). The following day the medium was aspirated and replaced with fresh medium containing puromycin (0.5 μg/mL) for selection of stable transfectants. Multiple individual ACTN1 shRNA clones were isolated and ACTN1 knockdown confirmed by SDS-PAGE immunoblotting, three representative clones were selected for further analysis.

To generate a 'rescue' ACTN1 vector, full length cDNA encoding ACTN1 was cloned in frame into the pEntr4 vector containing the GFP sequence (Clontech, Palo Alto, CA). The ACTN1 cassette was subsequently subcloned into the polylinker of the pENTR4 vector (Invitrogen). Four point mutations were created within the ACTN1 target shRNA sequence using a mutagenesis kit (Agilent Technologies, Santa Clara, CA). These point mutations conserved the amino acid sequence of ACTN1 and prevented the refractory construct from being targeted by RNAi machinery. The entry vector containing the refractory ACTN1 sequence was used in a LR recombination reaction with the pAD/CMV/V5-DEST vector (Life Technologies) to generate an expression clone. The expression clone was transfected into 293A cells using Lipofectamine 2000 (Life Technologies). After 10 days, the crude viral lysate was harvested and used to amplify the adenovirus. The amplified viral stock was titered and keratinocytes were infected at a multiplicity of infection of 1:50 in cell medium.

Human primary keratinocytes (pHEK) were isolated from de-identified discarded human foreskins obtained from routine circumcisions performed on neonates at Prentice women's hospital by the Northwestern University Skin Disease Research Center, Chicago, IL (Chicago, IL; IRB project no. STU00002257). Institutional approval nor patient consent was necessary. The isolated cells were maintained in culture as detailed previously (Hamill *et al.*, 2011b).

Antibodies

Rabbit polyclonal antibodies against ACTN1, ACTN4 and paxillin were purchased from Epitomics Inc. (Burlingame, CA, USA) and rabbit antibodies against lamin A/C were obtained from Cell Signaling (Beverley, MA, USA). Mouse monoclonal antibodies against β4 (3E1), α3 (P1B5) and α4 (6S6) integrin were purchased from Millipore (Billerica, MA, USA) while mouse monoclonal antibodies against talin and vinculin were obtained from Sigma-Aldrich (St Louis, MO, USA). Rabbit polyclonal antibody against phosphorylated FAK (Tyr397) was purchased from Abcam Inc. (Cambridge, MA). Rhodamine-conjugated phalloidin was purchased from Life Technologies. Monoclonal and polyclonal antibodies against collagen XVII have been described previously (Riddelle *et al.*, 1991). Secondary antibodies conjugated with various fluorochromes or horseradish peroxidase were purchased from Jackson ImmunoResearch Laboratories Inc. (West Grove, PA, USA).

SDS-PAGE and Western Immunoblotting

Cell extracts were derived as previously described (Langhofer *et al.*, 1993; Riddelle *et al.*, 1991) and then processed for SDS-PAGE and immunoblotting as described elsewhere (Harlow and Lane, 1999; Riddelle *et al.*, 1991). Western immunoblots were scanned and

quantified using a MetaMorph imaging system (Universal Imaging Corp.; Molecular Devices, Downington, PA) as defined elsewhere (Sehgal *et al*., 2006).

Immunofluorescence Microscopy

Cells were plated on glass coverslips and processed as previously described (Sehgal *et al*., 2006). The slides were imaged with a confocal scanning microscope (UV LSM 510; Zeiss Inc., Thornwood, NY or Leica SP8X, Leica Microsystems Inc., Buffalo Grove, IL). The images were exported as TIF files and processed using FIJI software (NIH). Focal adhesions were scored as either individual dashes or large arcs in images of cells prepared for immunofluorescence using antibodies against paxillin.

Observations of live cells, motility assays, kymography and scratch wound assays

Cell surface area, lamellipodial area and lamellipodia number were measured from individual cell images captured on a Nikon TE2000 inverted microscope (Nikon Inc., Melville, NY) and measured using MetaMorph software. For single cell motility and scratch assays, procedures were essentially as previously described in detail (Sehgal *et al*., 2006). For single cell motility studies, keratinocytes were plated on uncoated tissue culture plates 18–24 hours prior to the start of the assay. In some studies assays of motility were performed on cells plated onto the substrates coated with laminin-332 or fibronectin, purchased from Sigma-Aldrich, as detailed elsewhere. Assays were begun 6–10 hours after plating onto such coated surfaces. In all motility assays cells were imaged every 2 minutes over 1 hour and cell motility behavior was analyzed using MetaMorph software. For each cell line, means of speed (distance/time) and processivity (max distance from origin/total distance) were calculated. For kymography, cells were plated as above and images taken with a 60x objective every 5 seconds for 10 minutes. A kymograph was generated from a 1-pixel-wide line in the direction of migration was drawn on the resultant stack of images using MetaMorph software and measurements of lamellipodia extension distance and persistence were measured (Hinz *et al*., 1999).

To perform scratch wound assays, cells were grown to confluence and then a single wound was created in the culture using a yellow pipetteman tip. The culture was fed and then imaged immediately and at various times after wounding by phase contrast microscopy. The two edges of the wound in each image were outlined using ImageJ software (NIH) and the distance between the lines was measured along the entire length of the wound (a minimum of 500 measurements per wound). The average wound width was then determined either at 6h after wounding (primary cells in two trials) or at 12 and 24h after wounding (iHEK cells and clones in three trials for each cell type).

Fluorescence-activated cell sorting (FACS)

Freshly trypsinized cells were resuspended in PBS, containing 50% (v/v) normal goat serum, incubated with monoclonal antibodies against α3 integrin (P1B5) or β4 integrin (3E1) for 45 minutes at room temperature and then washed with PBS. As a control, primary antibody was omitted from the first incubation. Cells were then incubated with FITC-conjugated goat anti-mouse IgG for 45 minutes, washed with PBS and then resuspended in

PBS. A Beckman Coulter Elite PCS sorter (Beckman Coulter, Fullerton, CA) was used for analysis.

Fluorescence recovery after photobleaching (FRAP)

FRAP studies were performed as described elsewhere (Hamill *et al*., 2013; Tsuruta *et al*., 2002; Tsuruta *et al*., 2003). Time-lapse observations were made using a LSM 510 confocal microscope (Zeiss Inc.) under the following conditions: 100×, 1.4 numerical aperture oil immersion objective, maximum power 25 mW, tube current 5.1A (31% laser power), pinhole 1.33 airy units (optical slice 1.0 μm). GFP images were acquired by excitation at 488 nm and emission at 515–545 nm. Cell regions were bleached at the plane of the membrane at 488 nm, 100% laser power using the minimum number of iterations to cause complete bleaching (20–40). Recovery was monitored at 31% laser power at 1 minute intervals. For quantitative analyses, the fluorescence intensity of (1) the photobleached region, (2) the extracellular background intensity and (3) intracellular brightest intensity were determined using Metamorph 4.0 (Universal Imaging) software. All data were analyzed using Microsoft Excel. Data were adjusted for sample fading as detailed elsewhere (Hamill *et al*., 2013; Tsuruta *et al*., 2002; Tsuruta *et al*., 2003).

Supplementary Material

Refer to Web version on PubMed Central for supplementary material.

ACKNOWLEDGMENTS

Research reported in this publication was supported by the National Institute of Arthritis and Musculoskeletal and Skin Diseases of the National Institutes of Health under Award Numbers RO1 AR054184 and K99 AR060242. The content is solely the responsibility of the authors and does not necessarily represent the official views of the National Institutes of Health. We thank Dr. Peter Marinkovich for providing JEB cells.

Abbreviations

ACTN1	actinin-1
ACTN4	actinin-4
GFP	green fluorescent protein
iHEK	immortalized human keratinocyte
pHEK	primary human keratinocyte
JEB	junctional epidermolysis bullosa
shRNA	small hairpin RNA
FAK	focal adhesion kinase.

REFERENCES

Babakov VN, Petukhova OA, Turoverova LV, et al. RelA/NF-kappaB transcription factor associates with alpha-actinin-4. Exp Cell Res. 2008; 314:1030–1038. [PubMed: 18215660]

Baron MD, Davison MD, Jones P, et al. The sequence of chick alpha-actinin reveals homologies to spectrin and calmodulin. J Biol Chem. 1987; 262:17623–17629. [PubMed: 2826427]

Beggs AH, Byers TJ, Knoll JH, et al. Cloning and characterization of two human skeletal muscle alpha-actinin genes located on chromosomes 1 and 11. J Biol Chem. 1992; 267:9281–9288. [PubMed: 1339456]

Carter WG, Kaur P, Gil SG, et al. Distinct functions for integrins alpha 3 beta 1 in focal adhesions and alpha 6 beta 4/bullous pemphigoid antigen in a new stable anchoring contact (SAC) of keratinocytes: relation to hemidesmosomes. J Cell Biol. 1990; 111:3141–3154. [PubMed: 2269668]

Craig DH, Haimovich B, Basson MD. Alpha-actinin-1 phosphorylation modulates pressure-induced colon cancer cell adhesion through regulation of focal adhesion kinase-Src interaction. Am J Physiol Cell Physiol. 2007; 293:C1862–C1874. [PubMed: 17898132]

Dixson JD, Forstner MJ, Garcia DM. The alpha-actinin gene family: a revised classification. J Mol Evol. 2003; 56:1–10. [PubMed: 12569417]

Gluck U, Ben-Ze'ev A. Modulation of alpha-actinin levels affects cell motility and confers tumorigenicity on 3T3 cells. J Cell Sci. 1994; 107:1773–1782. [PubMed: 7983147]

Gonzalez AM, Otey C, Edlund M, et al. Interactions of a hemidesmosome component and actinin family members. J Cell Sci. 2001; 114:4197–4206. [PubMed: 11739652]

Hamill KJ, Hopkinson SB, Jonkman MF, et al. Type XVII collagen regulates lamellipod stability, cell motility, and signaling to Rac1 by targeting bullous pemphigoid antigen 1e to α6β4 integrin. J Biol Chem. 2011a; 286:26768–26780. [PubMed: 21642434]

Hamill KJ, Hopkinson SB, Hoover P, et al. Fibronectin determines skin cell motile behavior. J Invest Derm. 2011b; 132:448–457. [PubMed: 21956124]

Hamill KJ, Hopkinson SB, Skalli O, et al. Actinin-4 in keratinocytes regulates motility via an effect on lamellipodia stability and matrix adhesions. FASEB J. 2013; 27:546–556. [PubMed: 23085994]

Harlow, E.; Lane, D. Using antibodies : a laboratory manual. Cold Spring Harbor, NY: Cold Spring Harbor Laboratory Press; 1999.

Hinz B, Alt W, Johnen C, Herzog V, et al. Quantifying lamella dynamics of cultured cells by SACED, a new computer-assisted motion analysis. Exp Cell Res. 1999; 251:234–243. [PubMed: 10438589]

Honda K, Yamada T, Endo R, et al. Actinin-4, a novel actin-bundling protein associated with cell motility and cancer invasion. J Cell Biol. 1998; 140:1383–1393. [PubMed: 9508771]

Hynes RO. Integrins: Bidirectional, allosteric signaling machines. Cell. 2002; 110:673–687. [PubMed: 12297042]

Jones JCR, Hopkinson SB, Goldfinger LE. Structure and assembly of hemidesmosomes. BioEssays. 1998; 20:488–494. [PubMed: 9699461]

Khurana S, Chakraborty S, Cheng X, et al. The actin-binding protein, actinin alpha 4 (ACTN4), is a nuclear receptor coactivator that promotes proliferation of MCF-7 breast cancer cells. J Biol Chem. 2011; 286:1850–1859. [PubMed: 21078666]

Khurana S, Chakraborty S, Zhao X, et al. Identification of a novel LXXLL motif in alpha-actinin 4-spliced isoform that is critical for its interaction with estrogen receptor alpha and co-activators. J Biol Chem. 2012; 287:35418–35429. [PubMed: 22908231]

Kligys KR, Wu Y, Hopkinson SB, et al. α6β4 integrin, a master regulator of expression of integrins in human keratinocytes. J Biol Chem. 2012; 287:17975–17984. [PubMed: 22493440]

Kovac B, Teo JL, Makela TP, et al. Assembly of non-contractile dorsal stress fibers requires alpha-actinin-1 and Rac1 in migrating and spreading cells. J Cell Sci. 2013; 126:263–273. [PubMed: 23132927]

Langhofer M, Hopkinson SB, Jones JCR. The matrix secreted by 804G cells contains laminin-related components that participate in hemidesmosome assembly in vitro. J Cell Sci. 1993; 105:753–764. [PubMed: 8408302]

Martin P. Wound healing—aiming for perfect skin regeneration. Science. 1997; 276:75–81. [PubMed: 9082989]

Millake DB, Blanchard AD, Patel B, et al. The cDNA sequence of a human placental alpha-actinin. Nucl Acids Res. 1989; 17:6725. [PubMed: 2780298]

Otey CA, Pavalko FM, Burridge K. An interaction between alpha-actinin and the beta 1 integrin subunit in vitro. J Cell Biol. 1990; 111:721–729. [PubMed: 2116421]

Ozawa T, Tsuruta D, Jones JCR, et al. Dynamic relationship of focal contacts and hemidesmosome protein complexes in live cells. J Invest Dermatol. 2010; 130:1624–1635. [PubMed: 20107487]

Parr T, Waites GT, Patel B, et al. A chick skeletal-muscle alpha-actinin gene gives rise to two alternatively spliced isoforms which differ in the EF-hand Ca(2+)-binding domain. Eur J Biochem. 1992; 210:801–809. [PubMed: 1483465]

Quick Q, Skalli O. Alpha-actinin 1 and alpha-actinin 4: contrasting roles in the survival, motility, and RhoA signaling of astrocytoma cells. Exp Cell Res. 2010; 316:1137–1147. [PubMed: 20156433]

Riddelle KS, Green KJ, Jones JCR. Formation of hemidesmosomes in vitro by a transformed rat bladder cell line. J Cell Biol. 1991; 112:159–168. [PubMed: 1986003]

Riddelle KS, Hopkinson SB, Jones JCR. Hemidesmosomes in the epithelial cell line 804G: their fate during wound closure, mitosis and drug induced reorganization of the cytoskeleton. J Cell Sci. 1992; 103:475–490. [PubMed: 1478949]

Sehgal BU, DeBiase PJ, Matzno S, et al. Integrin β4 regulates migratory behavior of keratinocytes by determining laminin-332 organization. J Biol Chem. 2006; 281:35487–35498. [PubMed: 16973601]

Sen S, Dong M, Kumar S. Isoform-specific contributions of alpha-actinin to glioma cell mechanobiology. PloS one. 2009; 4:e8427. [PubMed: 20037648]

Stock EL, Kurpakus MA, Sambol B, et al. Adhesion complex formation after small keratectomy wounds in the cornea. Invest Ophthalmol Vis Sci. 1992; 33:304–313. [PubMed: 1740360]

Tsuruta D, Gonzales M, Hopkinson SB, et al. Microfilament-dependent movement of the β3 integrin subunit within focal contacts of endothelial cells. FASEB J. 2002; 16:866–868. [PubMed: 11967230]

Tsuruta D, Hopkinson SB, Jones JC. Hemidesmosome protein dynamics in live epithelial cells. Cell Motil Cytoskel. 2003; 54:122–134.

Underwood RA, Carter WG, Usui ML, et al. Ultrastructural localization of integrin subunits β4 and α3 within the migrating epithelial tongue of in vivo human wounds. J Histochem Cytochem. 2009; 57:123–142. [PubMed: 18824633]

Vallenius T, Luukko K, Makela TP. CLP-36 PDZ-LIM protein associates with nonmuscle alpha-actinin-1 and alpha-actinin-4. J Biol Chem. 2000; 275:11100–11105. [PubMed: 10753915]

Yamaji S, Suzuki A, Kanamori H, et al. Affixin interacts with alpha-actinin and mediates integrin signaling for reorganization of F-actin induced by initial cell-substrate interaction. J Cell Biol. 2004; 165:539–551. [PubMed: 15159419]

Youssoufian H, McAfee M, Kwiatkowski DJ. Cloning and chromosomal localization of the human cytoskeletal alpha-actinin gene reveals linkage to the beta-spectrin gene. Am J Hum Gen. 1990; 47:62–72.

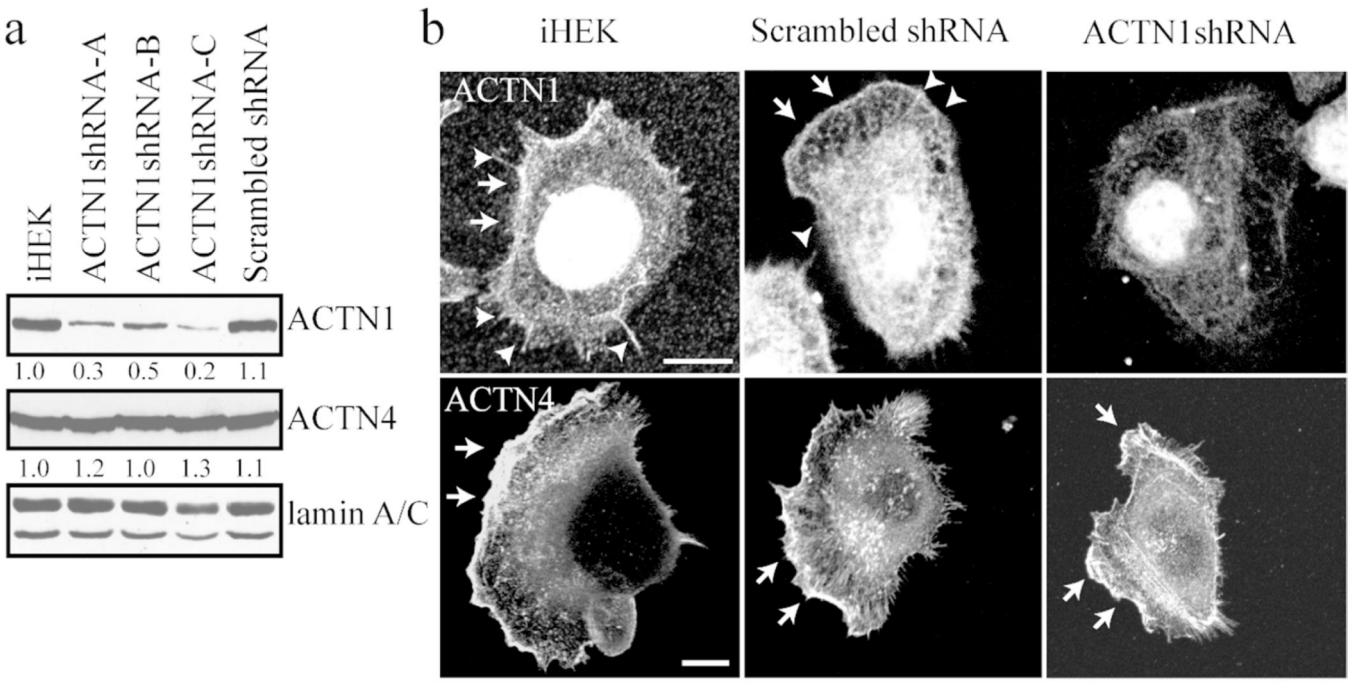

Figure 1. ACTN1 and ACTN4 expression and localization in keratinocytes

(**a**) Extracts of iHEKs, three clones of iHEKs infected with virus encoding ACTN1 shRNA (ACTN1shRNA-A, -B and -C) and iHEKs infected with virus encoding scrambled shRNA (scrambled shRNA) were processed for immunoblotting using antibodies against ACTN1, ACTN4 and lamin A/C as indicated. Lamin A/C reactivity was used as a loading control. Blots were scanned and quantified by densitometry, values were normalized to lamin A/C levels and are displayed relative to iHEKs levels. The blot is representative of at least three independent trials. (**b**) iHEKs, iHEKs expressing scrambled shRNA and iHEKs expressing ACTN1 shRNA were prepared for immunofluorescence staining either with ACTN1 antibodies (upper panels) or ACTN4 antibodies (lower panels). Note that the actinin-1 antibody stains the nucleus. This staining is not lost following actinin-1 knockdown indicating that it is non-specific. Arrowheads indicate filopodia and arrows lamellipodial extensions. Bars in images, 10 μm.

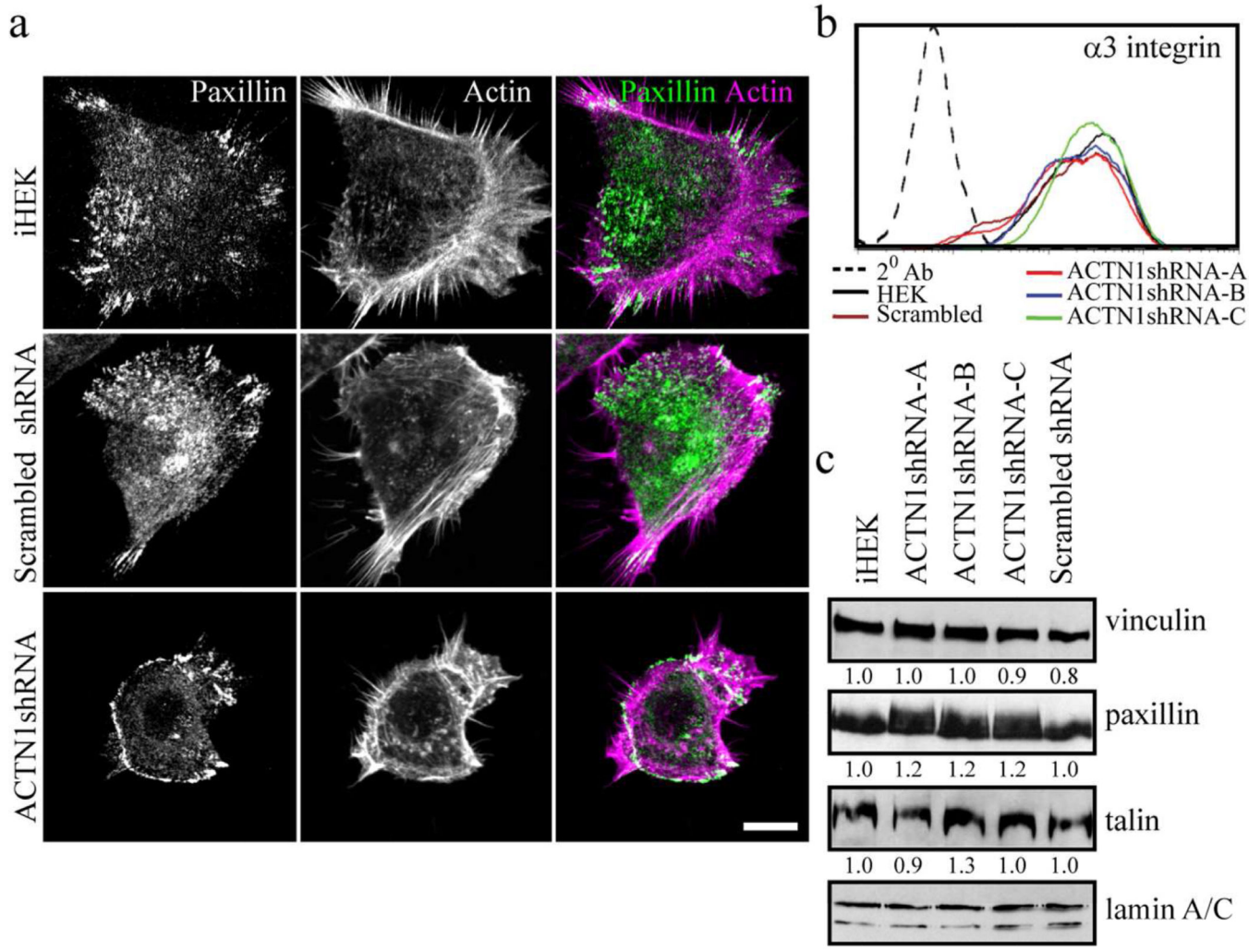

Figure 2. ACTN1 knockdown and effects on focal adhesion protein expression and localization

(**a**) iHEKs, iHEKs expressing scrambled shRNA and iHEKs expressing ACTN1 shRNA were prepared for immunofluorescence staining with antibodies against paxillin (left panels) and rhodamine phalloidin (middle panels)(only one knockdown clone is shown). Panels on right show overlays of the two images. Bar, 10 μm. (**b**) iHEKs, the three actinin-1 knockdown clones (ACTN1shRNA-A, -B and -C) and iHEKs expressing scrambled shRNA were prepared for FACS using antibodies against α3 integrin. 2^0 Ab indicates a control assay where primary antibody was omitted. (**c**) Extracts of the same cells as in **b** were processed for immunoblotting using antibodies against vinculin, paxillin, talin and lamin A/C as indicated. Lamin A/C reactivity was used as a loading control. Blots were scanned and quantified by densitometry, values were normalized to lamin A/C levels and are displayed relative to iHEKs levels. The blot is representative of at least three independent trials.

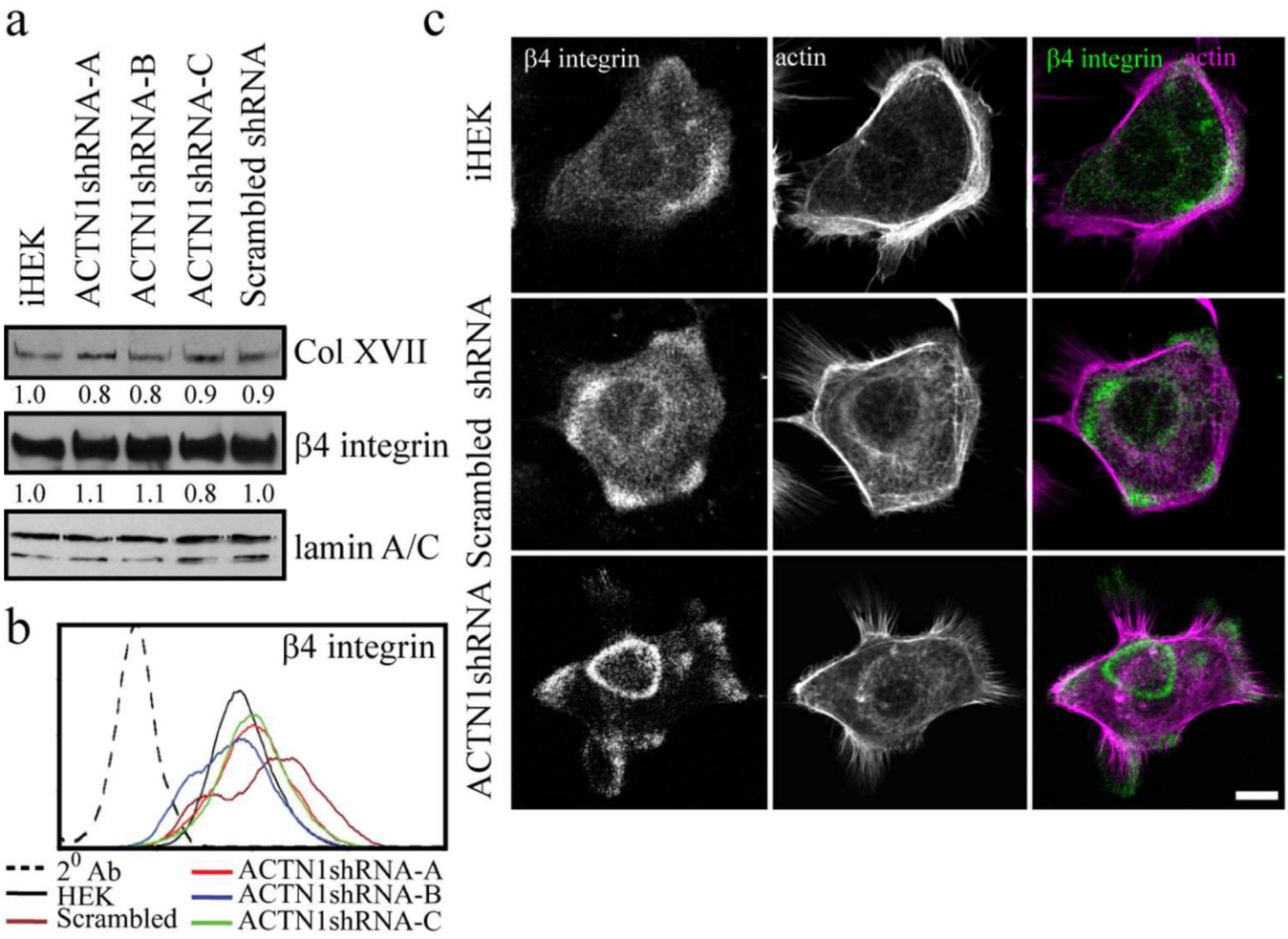

Figure 3. ACTN1 knockdown and effects on hemidesmosomal protein expression and localization

(**a**) Extracts of iHEKs, the three ACTN1 knockdown clones (ACTN1shRNA-A, -B and -C) and iHEKs expressing scrambled shRNA were processed for immunoblotting using antibodies against collagen XVII (Col XVII), β4 integrin or lamin A/C as indicated. Blots were scanned and quantified by densitometry, values were normalized to lamin A/C levels and are displayed relative to iHEK levels. Lamin A/C reactivity was used as a loading control. The blot is representative of at least three independent trials. (**b**) The same cells as in **a** were prepared for FACS using antibodies against β4 integrin. 2^0 Ab indicates a control assay where primary antibody was omitted. (**c**) iHEKs, iHEKs expressing scrambled shRNA and iHEKs expressing ACTN1 shRNA were prepared for immunofluorescence staining with antibodies against β4 integrin together with rhodamine phalloidin. Panels on right show overlays of the two images. Bar, 10 μm.

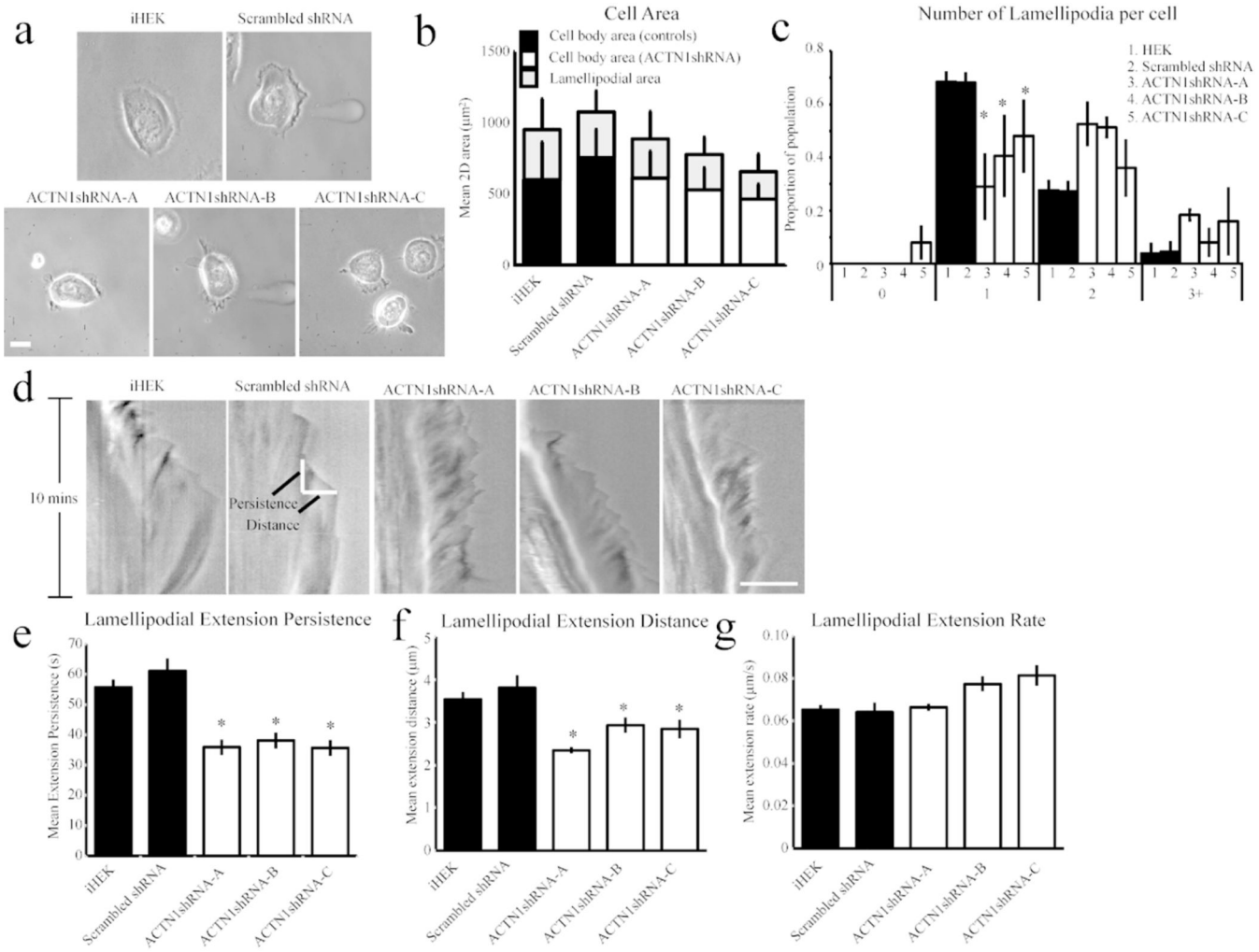

Figure 4. ACTN1 knockdown impacts lamellipodial dynamics

(**a**) Representative phase-contrast images of iHEKs, iHEKs expressing scrambled shRNA and the three ACTN1 knockdown clones plated overnight on glass bottomed dishes. (**b**) Mean ± s.e. cell body and lamellipodial area determined from images from 3 independent experiments, 50–100 cells/group. (**c**) Cells were scored based on the number of lamellipodial protrusions and plotted as percentage of the population displaying 0, 1, 2, or 3+ lamellipodia. (**d–g**) Phase contrast images of cells were captured every 5s over 10mins and kymographs generated as a montage of the pixels beneath a line drawn in the direction of the largest lamellipodial protrusion. (**d**) Representative kymographs from each cell line with time on the vertical axis. Example measurement sites of extension persistence (time spent in elongation phase) and extension distance (length of extension from base of previous retraction event) are indicated. Mean ± s.e plots of extension persistence (**e**), extension distance (**f**) and extension rate (**g**). Plots are derived from 25–50 cell/line in three independent studies. Bars in **a** and **d**, 10 μm. In **c**, **e** and **f**, * denotes significant differences from iHEK and scrambled shRNA controls groups as determined by ANOVA, $p<0.05$.

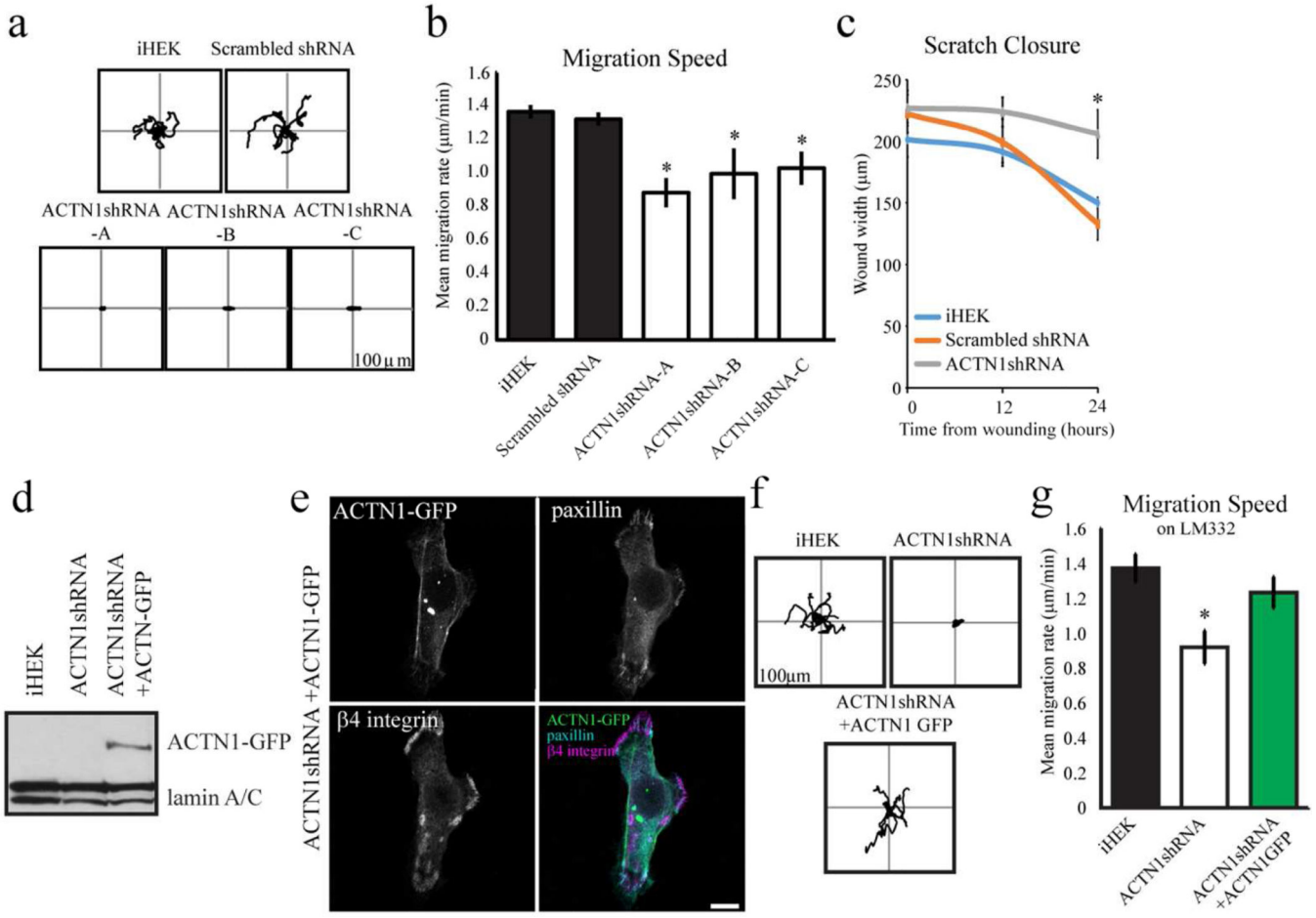

Figure 5. ACTN1 knockdown impacts cell motility

(**a**) Representative rose diagrams depicting the motility behavior of iHEKs, iHEKs expressing scrambled shRNA and the three ACTN1 knockdown clones (ACTN1shRNA-A, -B and -C). The cells were viewed over a 1 hour period, 18–24 hours after plating onto uncoated substrates. In **b**, the migration speed of the cells in (**a**) is depicted graphically. * Denotes significant differences, p>0.05. (**c**) At time 0, linear scratchs were introduced into confluent monolayers of iHEKs, iHEKs expressing scrambled shRNA and one ACTN1 knockdown clone. The scratch width was measured at indicated points. * Denotes significant difference, p<0.05, from both iHEK and scrambled shRNA. In **d**, extracts of iHEKs, iHEKs expressing ACTN1 shRNA cells and the latter cells induced to express GFP-tagged actinin-1 mRNA refractory to ACTN1 shRNA were prepared for immunoblotting using antibodies against GFP and lamin A/C. The latter serve as a loading control. (**e**) iHEKs expressing ACTN1 shRNA and the GFPtagged ACTN1 as in **c** were viewed by confocal fluorescence microscopy using antibodies against paxillin and β4 integrin, in combination with direct visualization of GFP, as indicated. The panel in the lower right is an overlay of all three images. Bar, 10 µm. (**f**) Rose diagrams depicting the motility behavior of representative iHEKs, iHEKs expressing ACTN1 shRNA and the latter cells induced to express GFPtagged ACTN1 mRNA refractory to ACTN1 shRNA are shown. The cells were plated onto iHEK matrix and allowed to adhere for 6–10 hours prior to being assayed for 1

hour. (**g**) Migration speed of the cells as in **e**. The results of quantification of GFPpositive cells only are shown for the 'rescued' cells (ACTN1shRNA + ACTN1GFP) in **e** and **f**. * Denotes significant differences between ACTN1 shRNA expressing cells and both iHEK and iHEK expressing scrambled shRNA (**b,c**) or between ACTN1 shRNA expressing cells and the same cells induced to express the GFP-tagged ACTN1 mRNA (**g**), $p<0.05$.

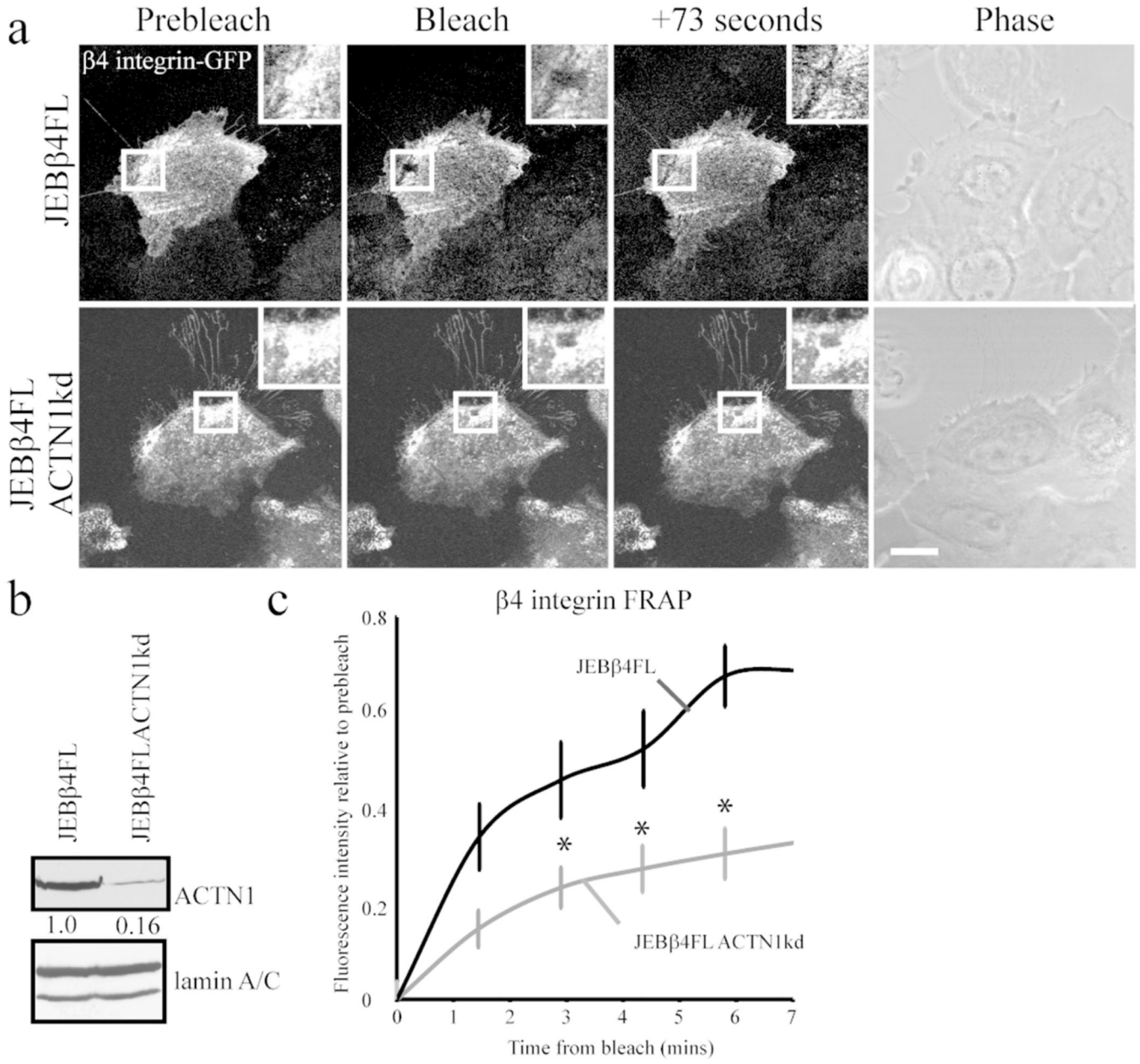

Figure 6. β4 integrin dynamics are reduced in ACTN1 knockdown keratinocytes

Junctional epidermolysis bullosa keratinocytes expressing fulllength β4 integrin tagged with GFP (JEBβ4FL) were infected with lentivirus encoding shRNA targeting ACTN1 (JEBβ4FLACTN1kd). Cells were plated at confluence onto glass-bottomed dishes then scratch wounded. Regions within organized β4 integrin GFP clusters were bleached 6h following wounding in cells at wound margins. (**a**) Representative images of prebleach, immediately following bleaching and at 73 seconds of recovery are displayed with a phase contrast image of cells. Bleach region is boxed in low power views and shown at higher magnification in inset. Bar, 10 μm. (**b**) Western immunoblot of total protein extracts were blotted with antibodies against ACTN1 and lamin A/C as indicated. Blots were scanned and quantified by densitometry, values were normalized to lamin A/C levels and are displayed

relative to JEBβ4FL levels. The blot is representative of at least three independent trials. (**c**) Mean ± s.e. percentage of pre-bleach level fluorescence recovery of each cell line was determined from >15 assays/line. * Denotes significant difference versus JEBβ4FL cells, $p<0.05$.